Density of states, level-statistics and localization of fractons in 2- and 3-dimensional disordered systems

P. Argyrakis[1], S.N. Evangelou[2], and K. Magoutis[1]

[1] Department of Physics 313-1, University of Thessaloniki, GR-54006 Thessaloniki, Greece
[2] Department of Physics, University of Ioannina, GR-45110 Ioannina, Greece

We calculate by the Lanczos method the density of spin wave states, and its fluctuation properties on the infinite percolating cluster of a randomly site-dilute Heisenberg ferromagnet. Our results demonstrate that the averaged density follows the fracton laws with spectral dimension values $d_s = 1.32$ and $d_s = 1.30$ in two and three dimensions, respectively, and is smooth at the magnon-fracton crossover. Similar laws are also shown in the case of continuous disorder on the bonds of the clusters. The density fluctuations are studied via the nearest energy-level-spacing distribution function $P(S)$, which is shown to obey the Wigner surmise with level-repulsion far from the percolation threshold p_c and an almost Poisson law with uncorrelated spectrum at p_c. The localization properties of excitations are investigated by considering the density of states fluctuations and also via the participation ratio of the eigenvector amplitudes. It is seen that the fracton states are sharply localized. Our results are further discussed in connection to previous theories and numerical data.

1. Introduction

Many disordered systems possess fractal scaling, at least up to a certain length scale [1]. One of the most studied examples is the random percolating cluster [2] realized on d-dimensional lattices, in which a fraction p of sites are randomly occupied and $1-p$ are empty. When p increases the mean cluster size increases and there is a critical percolation concentration p_c for $d > 1$ above which an infinite percolating cluster is formed. Exactly at the critical point the infinite percolating cluster is fractal. A characteristic percolation correlation length ξ_p exists, which is finite for p below and above p_c and diverges for $p = p_c$ via a dimensionality-dependent exponent ν. The probability that a given site belongs to the infinite percolating cluster $P(p)$ vanishes as $p \to p_c^+$ with an exponent β. The percolating cluster is a self-similar fractal object

in the statistical sense, characterized up to the correlation length ξ_p by a fractal dimension $d_f = d - \beta/\nu$ [1-3]. Estimates for the geometrical exponents ν, β and the fractal dimension d_f can be found in [3] for the various space dimensions $d > 1$.

The developments in this subject, during the last decade, concern not only the purely geometrical static, but also the dynamical properties of percolating structures. The most important results are summarized in the presence of anomalous slow diffusion and the introduction of the concept of fractons [4]. This is known as the dynamical scaling approach and these findings are directly relevant for the corresponding problem of the quantum eigensolutions arising from the Schrodinger equation defined on fractal structures. For one-magnon excitations [5] the scaling theory implies for $p = p_c$ a universal law for the density of states (DOS)

$$\langle \rho_{\mathrm{fr}}(E) \rangle \propto E^{d_s/2 - 1}, \tag{1}$$

when E is small, where the exponent d_s is the fracton dimension [4]. If equation (1) is compared to the usual magnon DOS

$$\langle \rho_{\mathrm{mg}}(E) \rangle \propto E^{d/2 - 1}, \tag{2}$$

d_s replaces the space dimension d. The Alexander-Orbach conjecture in any Euclidean dimension $d \geq 2$ [4] further predicts $d_s \simeq 4/3$; that is, d_s approximately takes a value close to its mean-field value. The phonon DOS is obtained if $E = -\omega^2$ and the expressions corresponding to (1) and (2) are $\propto \omega^{d_s - 1}$ and $\propto \omega^{d - 1}$ respectively.

For concentrations p above p_c the DOS consists of a small-E (long wavelength) magnon regime separated by a crossover region around a characteristic energy E_c, from a larger-E (shorter wavelength) fracton regime. The crossover between the two regimes was found in numerical calculations [6,7] to be smooth, unlike the original predictions of effective medium treatments for the existence of a peak at E_c [8]. The spin-wave studies should

also apply to the problem of vibrations [9] and classical diffusion [3] in disordered media, where most experimental data can be found [10, 11].

The localization properties of excitations when the underlying lattice is the percolating cluster, have also attracted considerable interest [12–14]. It is natural to expect that the topological disorder, due to the percolating cluster geometry, will drastically affect not only the spectral but also the transport properties of magnons, in a way similar to what disorder does to electron in metals. The localization phenomenon for electronic systems implies a drastic departure from the conventional Bloch theory, and mobility edges may appear in the electronic spectrum separating extended states, having constant amplitude on the average, from localized states that usually decay exponentially. However, it turns out that localization on percolating clusters is more intricate, since the "disorder" is due to the presence of self-similar fractal geometry. Strong localization on special parts of the percolating cluster was first found on the related quantum percolation model [13] and recently it was shown that super-localization [14], with decay faster than exponential, may occur, at least for typical samples before averaging.

The concern of this paper is the study of the DOS and the localization properties of magnons (or phonons) in percolating clusters generated in 2- and 3-dimensions. Our aim is to study the properties of fractons, also by going beyond an averaged picture, i.e. by considering the corresponding statistics of the eigensolutions. This is achieved via the introduction of a random matrix ensembles consisting of sparse Hamiltonian matrices which is appropriate to discuss fractons. The random matrices for the problem considered in this paper are short-ranged and very sparse, i.e. with most of the matrix elements being identically zero.

Exactly solvable random matrix ensembles have been introduced a long time ago by Wigner and Dyson, in the context of nuclear physics [15]. They consist of matrices with all their matrix elements being independent Gaussian random variables. For Gaussian ensembles the averaged DOS takes a simple semicircular form. The corresponding DOS-fluctuations are usually estimated by the distribution function $P(S)$ of the nearest-eigenvalue spacings S, which is the simplest measure of the fluctuations. For the Gaussian ensembles $P(S) \propto S$, for small S, which implies strongly correlated eigenvalues repelling their closest neighbours [15]. The exact result for $P(S)$ from the Wigner-Dyson theory (see (5) below) is known as the Wigner surmise [15]. Within the same theory the statistics of the eigenvector amplitude components can be also found [15]. The eigenstates are always extended (delocalized) and their statistics is characterized by the squared gaussian χ^2-distribution law.

From the previous discussion the Wigner surmise and the level-repulsion can be associated with the delocalized part of the spectrum in the presence of disorder. This is a consequence of the fact that the Gaussian matrix ensembles correspond to high-dimensionality lattice systems where no localization is found. The Wigner-Dyson statistics also turns out to be responsible for the meso-

scopic physics fluctuation phenomena which occur in small metallic samples [16]. On the other hand for low-dimensionality localized states exist and the level spacings are distributed according to a Poissonian law which permits clustering of eigenvalues [15]. From these observations it follows that the spectral fluctuation properties for disordered systems of intermediate dimensions can be used to distinguish between the two kinds of states. Therefore, the DOS fluctuations studies should permit the identification of the Anderson transition and the determination of mobility edges in the spectrum.

Since analytical solutions do not exist for disordered 2- and 3-dimensional systems we have used the Lanczos method [17] for computing numerically the eigenvalues and eigenvectors in our matrix ensembles. Firstly, we considered the question of fracton and magnon-fracton DOS for the percolating cluster at p_c and above p_c, respectively. Then the level-spacing distribution function $P(S)$ is determined so that the transport properties are directly estimated from the corresponding DOS-fluctuations. We present results which demonstrate two different kinds of behavior for the spectral fluctuations refering to uncorrelated and correlated spectra, respectively. A study of fracton mode amplitudes has also been carried out in order to measure their spatial extend. Finally, in order to simulate more realistic situations continuous disorder is added on the cluster bonds. Our findings are discussed in connection to previous studies and conclusions are drawn in Sect. 5.

2. The model and the method of calculation

We start from the familiar magnon equations of motion [5] corresponding to a single spin deviation on the incipient percolating cluster. They are

$$(E - \sum_{r'} J_{r,r'}) \Psi_r = \sum_{r'} J_{r,r'} \Psi_{r'}, \tag{3}$$

where r labels the percolating cluster sites on the d-dimensional lattice, E is the magnon energy and when E is an eigenvalue Ψ_r is the corresponding wavefunction amplitude on site r. J is the exchange constant and the summations are performed over all available sites r', nearest-neighbours of r. The exchange couplings $J_{r,r'}$ can be conveniently chosen to be 1, which sets the energy scale, except at Sect. 4, where the J's for every pair of sites are chosen to be uniformly distributed independent random variables.

From Eq. (3) the dynamical matrix $\mathbf{H}$ can be defined in the chosen orthogonalized site basis representation. $\mathbf{H}$ has off-diagonal matrix elements (bond strengths) 1 or 0, when nearest neighbour sites are present or absent, respectively. The diagonal elements (site energies) are equal to the number of nearest-neighbor sites of r present, ranging from 1 to $2d$. The model has a special form of correlation between diagonal and off-diagonal disorder and can be derived from a general tight-binding Hamiltonian. The resulting gapless spectrum consists of strictly positive energies in the range $0 \leq E \leq 12$. The $E = 0$ mode

must be extended for $p \geq p_c$, due to the continuous degeneracy of the ground state.

In our calculations the infinite percolating cluster at a given value of the concentration p was generated on large square $L \times L$ in $d = 2$, and cubic $L \times L \times L$ lattices in $d = 3$. We used the algorithm described in [18, 19] with periodic boundary conditions imposed in all directions. At the critical concentration p_c the clusters contained only a small fraction of the total number of lattice sites and the corresponding one-magnon Hamiltonians are set-up and diagonalized numerically. The statistical ensemble consists of large real, symmetric sparse matrices, i.e. each row or column has at most 5 non-zero elements in $d = 2$ and 7 elements in $d = 3$.

For the numerical diagonalization it is convenient to employ the Lanczos algorithm of Parlett and Reid [17] by making use of the matrices sparse nature. Using this method we compute part of the eigensolutions (eigenvalues and eigenvectors) which lie in a given energy interval. The method is repeated so it can cover the eigensolutions in the whole energy domain. The Lanczos method has been successfully used in similar kind of problems [20, 21]. A related method based on a reassessment of the original algorithm can be used only for the approximate determination of the local DOS and has become known as the recursion or tridiagonalization method [22]. For the DOS a most convenient and very accurate alternative computational technique can be used. It is known as the Gaussian elimination or triangularization method and was introduced in [6].

The main advantage of the Lanczos method is economy of storage, since **H** need not be stored. The storage requirements increase linearly with the matrix size N, since the computer memory contains only the non-zero matrix elements. In fact the product of **H** with an arbitrary vector **u** is all what is needed in the algorithm. It is also possible within the Lanczos method, after eigenvalues have converged, to evaluate the corresponding eigenvectors, which have also been computed within our approach. Although, the Lanczos method is superior to all other standard methods, as well as the variants which exploit the sparse matrix nature, it suffers from certain drawbacks. The most serious is the danger of duplicate eigenvalues. This is avoided in our routine which is based on the Harwell version of the algorithm. Unfortunately, as a consequence the method fails to distinguish between degenerate eigenvalues. Although, the problem considered in this paper contains many degenerate eigenvalues, e.g. in $d = 3$ at $p = p_c$ almost 17% of the total number of eigenvalues lie at $E = 0$. This difficulty does not affect our results which concern only the continuous part of the DOS.

A sufficient explanation for the origin of the special degenerate states is given in [13] on the related quantum percolation model. They correspond to "molecular states" localized in special parts of the infinite percolating cluster and they give rise to prominent δ-function peaks in the DOS which lie at $E = 0, 1, \sqrt{2}$, etc. They can be easily enumerated so that their degeneracy ratio can be determined [13, 21]. Our calculations do not include these states, but focus instead on the continuous features of the DOS related to magnons and fractons.

3. Calculations and discussion of the results

3.1. Densities of states (DOS)

The calculation of the DOS for a particular value of p proceeds as follows: We collect all the eigenvalues in energy bins (in histogram form) for many different, randomly generated clusters, so that the average $\langle \rho(E) \rangle$ can be determined. The sources of error in this type of calculation are twofold: Firstly, due to the finite number of samples making up our statistical ensemble a statistical error exists. This can be estimated from the scatter of the number of eigenvalues in a given energy bin. From ordinary statistics it is expected that for an energy bin containing n states we must have a statistical uncertainty of the order of $\sqrt{n}$. In fact if the mean number of eigenvalues in a given bin of width E is $\langle n(E) \rangle$ then the variance $\langle (\delta n(E)^2 \rangle = \langle (n(E))^2 \rangle - \langle n(E) \rangle^2$ is proportional to the mean $\langle n(E) \rangle$. This is a result of ordinary Poisson statistics which corresponds to localized states and the DOS fluctuations are very large. For delocalized states instead $\langle \delta n(E)^2 \rangle$ is much lower than $\langle n(E) \rangle$, varying logarithmically with $\langle n(E) \rangle$, as a result of the Wigner-Dyson theory [23].

In Ref. 23 the variance $\langle (\delta n(E))^2 \rangle$ is found to be equal to $\langle n(E) \rangle$ when the states in the bin are localized, much smaller than $\langle n(E) \rangle$ when are delocalized, and proportional to $\langle n(E) \rangle$ but with a proportionality index less than $1 (\sim 1/2)$ when the states are critical. Therefore, this statistical error is significant only for the localized fracton states and has been minimized by taking a rather large number of samples.

The second kind of error is due to the finite size of the chosen sample which results in a limited number of sites in a given energy bin. The average level spacing is $\propto (\langle \rho(E) \rangle N)^{-1}$, where N is the total number of eigenvalues, so that when N is not large enough the spectrum will show pronounced discreteness. This kind of error also limits us to extend the calculation down to very small energies. For the system sizes considered we have found large number of eigenvalues for $E \geq 0.001$. Both types of error have been monitored in our calculations by choosing large enough and many random clusters so that the combined error remains no more than within a few percent.

We report numerical results for the DOS at various p's above p_c in Figs. 1 and 2 for $d = 2$ and $d = 3$, respectively. It can be seen that for $p = p_c$ according to (1) the fracton singularity is seen for small E. For higher p values the low-energy regime corresponds to magnons (Eq. (2)) and a smooth magnon-fracton crossover around an energy E_c must be seen. Since the fracton edge E_c values are very close to zero and the magnon regime is not fully visible in Figs. 1, 2 we choose to plot the averaged integrated density of states (IDOS) against E by including a range of small energies. In the double logarithmic plot of Fig. 3 at $p = p_c$ the fracton law of eq. (1) implies that the data should be straight lines with gradient $d_s/2$. Despite the sources of error the data of Fig. 3 lie rather accurately on a straight line. A least-squares fit gave a gradient from which the exponent d_s is estimated as 1.32 ± 0.02 and
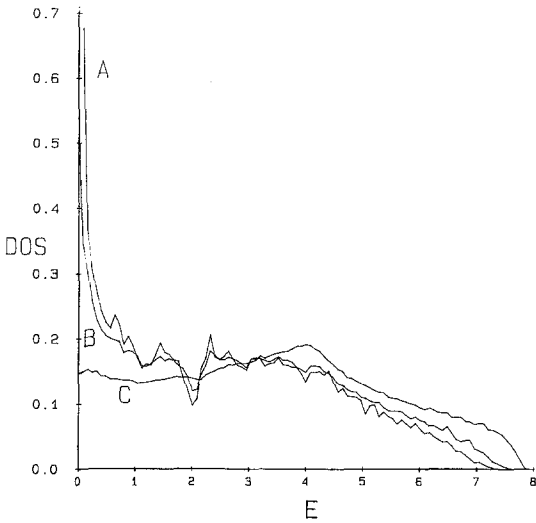
260

Fig. 1. Plot of the averaged DOS$\langle\rho(E)\rangle$ in 40×40, 2-dimensional lattice for three different values of p: (A)$p=p_c=0.5931$ from 100 clusters, (B)$p=0.69$ from 100 clusters and (C)$p=0.85$ from 20 clusters

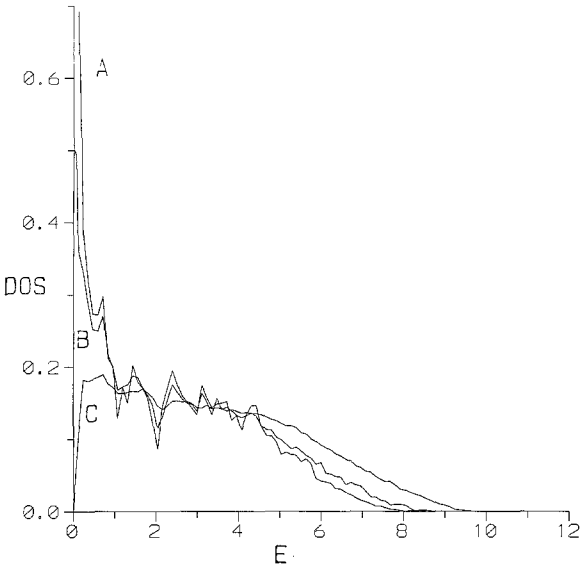**Fig. 3.** Plot of the averaged integrated density of states (IDOS) $\langle N(E)\rangle$ vs Energy E at $p=p_c$ for $d=2$, 3 in a log-log paper. The extracted values for the fracton exponent are: $d_s=1.32$ and 1.30 in $d=2$, 3, respectively. The capital D on the figure are simply the dimensionalities

Fig. 2. The same as Fig. 1 but for $20\times20\times20$ lattice in $d=3$: (A)$p=p_c=0.3117$ from 40 clusters, (B)$p=0.40$ from 10 clusters and (C)$p=0.55$ from 20 clusters

Fig. 4. The same as Fig. 3 but for p values above p_c. For $d=2$, $p=0.69$, average over 100 clusters, and for $d=3$, $p=0.40$, average over 10 clusters. The capital D on the figure are simply the dimensionalities

1.30 ± 0.02 in $d=2$, 3, respetively. We have also considered systems of smaller size which allowed us to estimate the corresponding finite size errors, which for the above values are about ±0.02. For not very large values of p above p_c, the two excitation regimes magnon and fracton are obtained in Fig. 4 for $d=2$, 3. The corresponding exponents from Eqs. (1, 2) are approximately $d/2$ (for magnons) and $d_s/2$ (for fractons). This gives 2/2, 3/2 for $d=2,3$ for magnons, and 2/3 for fractons. It can be clearly seen that our results displayed in Fig. 4 indicate the absence of a peak at the crossover, as it was firstly shown in numerical calculations for $d=2$ in [6].
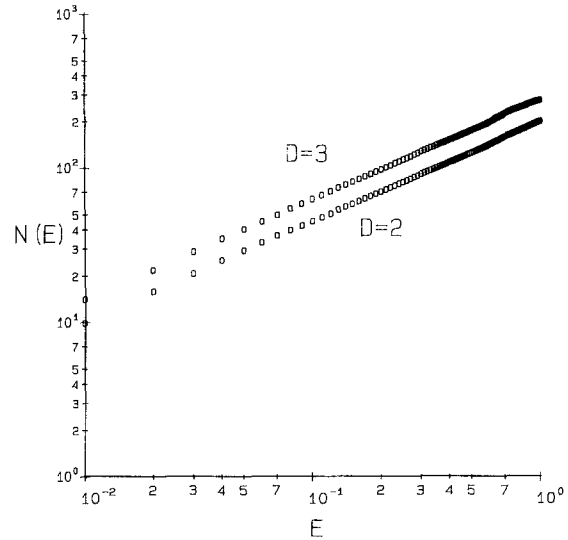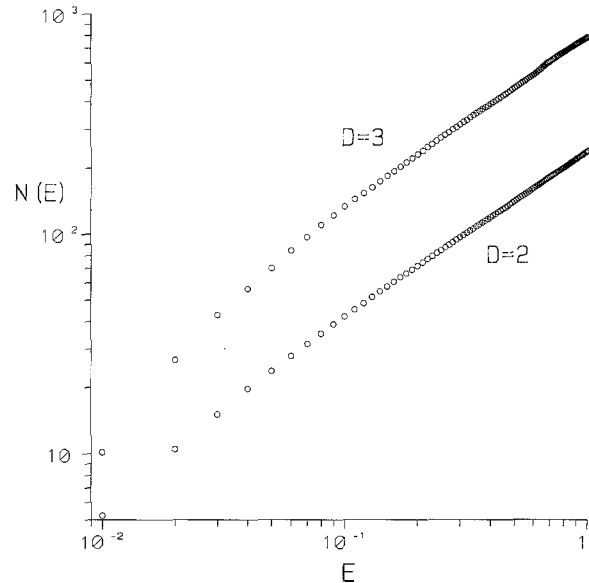
The previous results confirm the dynamical scaling approach of Alexander-Orbach [4], as summarized by (1), (2). A dispersion law different from quadratic $E\propto k^2$ is implied for fractons, at p_c, i.e.

$$E\propto k^{d_w}, \qquad k\xi_p\to0. \tag{4}$$

From the condition $k\xi_p\simeq0$ which gives $E_c\propto\xi_p^{-d_w}$ we can determine the crossover region. Therefore, the crossover energy E_c should scale as $(p-p_c)^{vd_w}$, giving approximately [10] $E_c\simeq0.03$ at $p=0.69$ in $d=2$, and $E_c\simeq0.08$ at $p=0.40$ in $d=3$, values appropriate for Fig. 4. Our find-

ings for the magnon exponents are 0.98 and 1.18 instead of $d/2 = 1$ and 1.5, in $d = 2$, 3, respectively. These deviations can be understood as arising from the numerical difficulties due to the very small energy values corresponding to the magnon regime.

The independent estimates for d_w which come from decimation and simulation data give approximately the best known values [3] as $d_w \simeq 2.87$ in $d = 2$ and $d_w \simeq 3.68$ in $d = 3$. Using also the known fractal dimensions $d_f = 91/48$ and $d_f = 2.53$ in $d = 2$, 3, respectively, we arrive from $d_s = 2 d_f / d_w$ at the values of the fracton exponent $d_s \simeq 1.32$ and $d_s \simeq 1.38$ in $d = 2$, 3 respectively. It can be concluded that our independent directly obtained data confirm both these estimates and also the universal value of 4/3, at least approximately. Our d_s values are found to be systematically slightly less in $d = 3$ than in $d = 2$ (see also Sect. 5) but support the Alexander-Orbach conjecture within the reported error bounds.

3.2. Level spacing distribution function $P(S)$

For localized states the corresponding spectra are uncorrelated and obey normal statistics while for delocalized states the Wigner-Dyson statistics is expected with smooth, correlated spectrum exhibiting level-repulsion and spectral rigidity. We considered the most common spectral fluctuation measure, the nearest-level spacing distribution function $P(S)$. For the Wigner-Dyson statistics in the case of real and symmetric random matrices (orthogonal ensemble) the well-known Wigner surmise law for delocalized states is

$$P(S) = (\pi S/2)\exp(-\pi S^2/4),\qquad(5)$$

which is in contrast to the usual Poisson law

$$P(S) = \exp(-S),\qquad(6)$$

expected for localized states.

We have studied the distribution function $P(S)$ of the nearest-energy-level spacings $S_n = E_{n+1} - E_n$ for various p values. The calculations are done by obtaining the eigenvalues for many random runs; the total number being approximately 70 000 and subsequently deconvoluting the spectrum [24], in order to retain a constant DOS. This is equivalent to studying the distribution of the difference

$$\langle \mathcal{N}(E_{n+1})\rangle - \langle \mathcal{N}(E_n)\rangle = (E_{n+1} - E_n)\frac{\partial}{\partial E}\langle \mathcal{N}(E)\rangle,$$

where $\langle \mathcal{N}(E)\rangle$ is the averaged IDOS at energy E. The results in $d = 3$ for $p = p_c$ and $p = 0.70$ are displayed in Fig. 5. For $p = 0.70$ they compare reasonably well with the corresponding Wigner surmise (Eq. (5)) suggesting that all states have become delocalized at this concentration. This is also consistent with a quantum percolation threshold p_q value smaller than 0.70 in $d = 3$. The fracton states at p_c instead follow a distribution rather close to a Poisson (Eq. (6)). The agreement, especially for the localized fracton case, would possibly be improved if more samples are included.
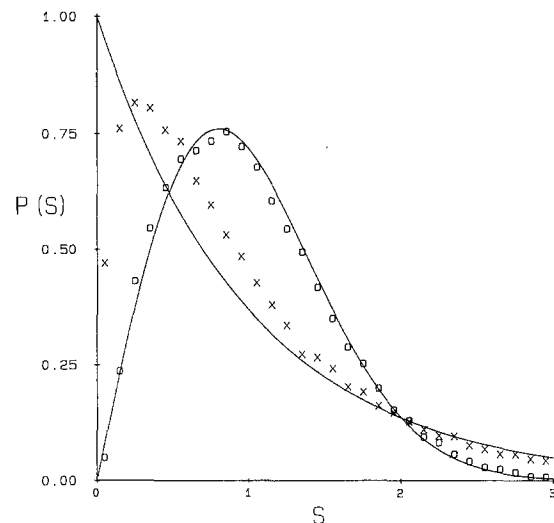

Fig. 5. The calculated level-spacing distribution function in $d = 3$ for $p = p_c$ (x's) and $p = 0.70$ (circles). The data are for 100 clusters in the full energy-range. The horizontal line is in units of the local mean-level spacing and the solid curves are the Wigner surmise and the Poisson law, respectively
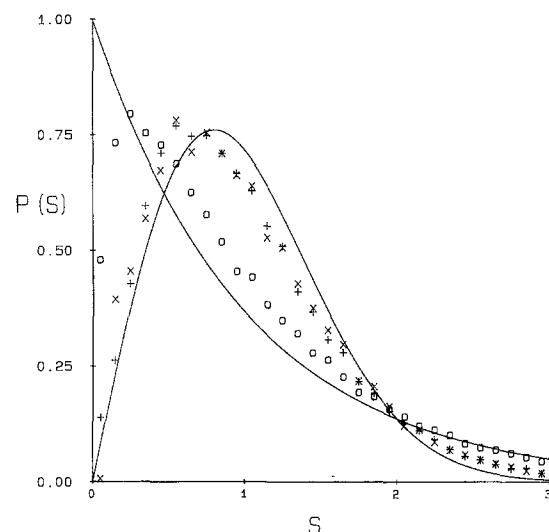

Fig. 6. The same as in Fig. 5 but for $p = 0.45$ in $15 \times 15 \times 15$ lattices. The x's concern statistics on the energy range [0, 1], the crosses on [3, 4] and the circles on [6, 7]

In Fig. 6 we examine in $d = 3$ an intermediate p case in an attempt to locate the mobility edge by studying energy-level statistics for three different parts of the spectrum. The obtained results for $p = 0.45$ suggest that a mobility edge must lie between $E = 4.0$ and 6.0. Since the fracton edge at this concentration lies at a much lower energy value ($E_c \simeq 0.40$) the estimated mobility edge clearly does not coincide with the fracton edge. The fracton states which should exist in the intermediate energy region between E_c and 6.0 appear as having localization lengths larger than the system size. In this calculation only the states near the tail of the spectrum have reached convergent localization lengths. These results imply the invalidity of the dynamic scaling theory accompanied by

the absence of fracton modes for p much larger than p_c. In this case the geometrical disorder, estimated from the deviation of p from the pure limit $p=1$, is just too weak to localize the excitations apart from the states which lie near the tail of the DOS.

3.3. Properties of eigenvectors

The localization properties can be directly probed by studying the eigenvector corresponding to the j-th eigenvalue. A common localization measure is the inverse participation ratio (IPR) [25], defined as

$$\text{IPR}(E_j) = \sum_{r=1}^{N} |\Psi_r^{(j)}|^4, \tag{7}$$

for the normalized eigenvector $\Psi_r^{(j)}$ corresponding to the eigenvalue E_j. If a state is localized on m sites then the IPR takes a value of order $1/m$. Therefore, when the IPR is significantly larger than $1/N$, where N is the total number of sites of the cluster considered, then the state is localized. The scaling theory [4] predicts the existence of a single averaged localization length for fractons. This implies that for a given system size the average $\langle \text{IPR} \rangle$ should vary with E as $E^{d_s/2}$.

The variations of IPR with energy near $E=0$ at p_c are shown on a logarithmic paper in Fig. 7. It can be seen that the fracton states are strongly localized but with localization lengths increasing as the energy lowers. Moreover, the IPR is not a self-averaging quantity [25] dominated by large fluctuations. The straight line on Fig. 7 is the fracton scaling law with a value $d_s \simeq 1.12$, which demonstrates the scaling behaviour for the averaged values.
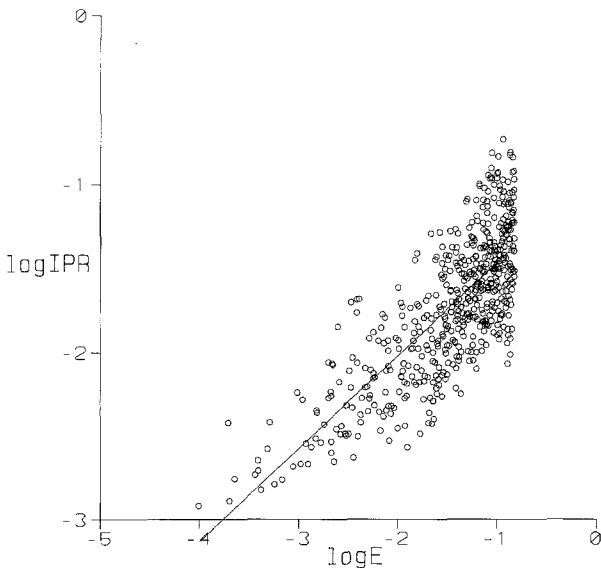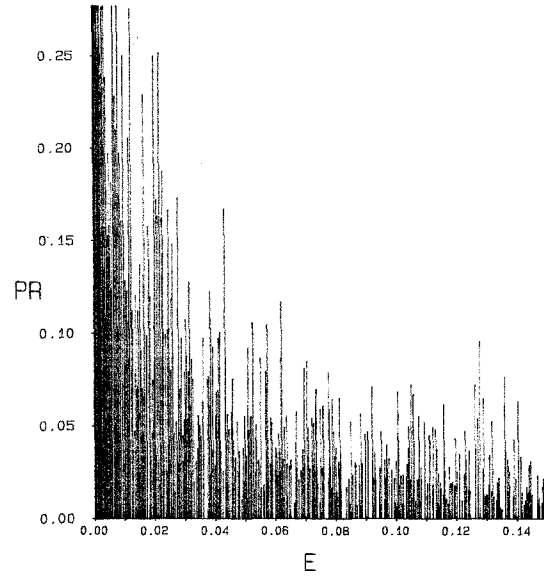

Fig. 8. The same as in Fig. 7 but for the PR in a linear scale

The participation ratio (PR) plotted versus energy E on Fig. 8 denotes the ratio of the number of sites with significant amplitude to the total number of sites. Our results of this section are not incompatible with the fracton scaling prediction although we must stress the fact that the mean values do not characterize the system due to the presence of large fluctuations, already apparent in Figs. 7 and 8.

We have also briefly addressed the more difficult question of super-localization, firstly proposed in [14]. It was argued that the wavefunction amplitude will decay with distance as $\exp(-c(E) \cdot r^{d_\phi})$, where d_ϕ is larger than 1. There exists a current debate whether $d_\phi = 1$ (which implies ordinary localization) or $d_\phi > 1$ (super-localization) with the most thorough investigation made by [26]. It was shown there that the ensemble averaged individual wavefunction amplitude realization decays with an exponent $d_\phi \simeq 2.3$, a value larger than theoretical estimates. The constant $c(E)$ is the inverse localization length raised to the power d_ϕ which turns out to satisfy closely the proportionality relation $E^{d_\phi \, d_s/(2 \, d_f)}$ and also implies scaling according to the fracton dispersion law [4]. We have not being able to answer the question of super-localization although we observed very sharp decay properties of the fracton amplitudes for particular realizations, indicating "molecular states" [26]. Moreover, by following the IPR for such modes and varying the system size we found very little size-dependence, which also implies strong localization.

Fig. 7. Logarithmic plot of the IPR against energy near $E=0$ for fracton states in $20 \times 20 \times 20$ lattices at $p=p_c$. Values of IPR for five eigenstates are superimposed. These states are localized, since IPR $\geq 1180^{-1}$ where 1180 is the total averaged number of sites. The straight line implies a fracton scaling law with $d_s \simeq 1.12$

4. Percolating clusters with random bonds

We have also considered a more general situation by including continuous randomness on the off-diagonal matrix elements. This should represent a more realistic situation; an extension corresponding to a percolating
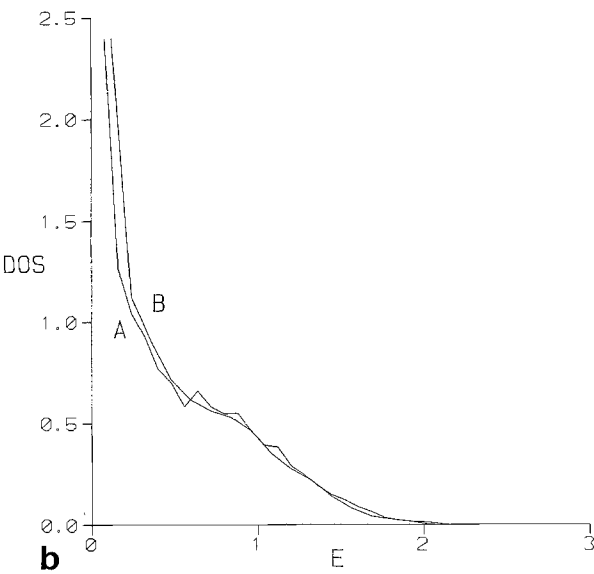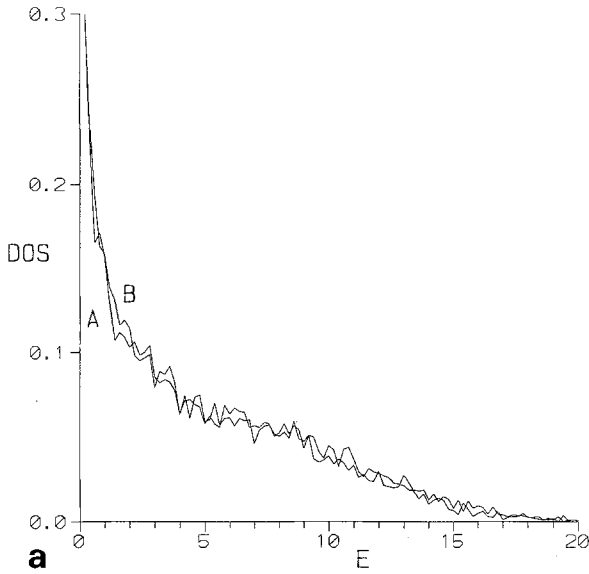
Fig. 9a, b. Plot of the averaged DOS$\langle \rho(E) \rangle$ in 40×40, 2-dimensional lattice for added continuous disorder of strength **a** $W=1$, **b** $W=10$

Fig. 10. Plot of the averaged integrated density of states $N(E)$ vs energy E at $p = p_c$ for $d = 2, 3$ in a log-log paper and $W = 1, 10$. The extracted values for the fracton exponents when $W = 1$ are: $d_s = 1.20$ and 1.16 in $d = 2, 3$ and for $W = 10$: $d_s = 1.31$ and 1.27 in $d = 2, 3$, respectively. The capital D on the figure are the dimensionalities

cluster with added bond-disorder. The fundamental question in this case is whether the fracton scaling laws will persist, despite the added non-geometrical disorder.

We chose the bond strengths from a uniform distribution between $[-W/2, W/2]$ and worked at $p = p_c$, both in $d = 2, 3$, for two values of disorder: $W = 1$ and 10. The results are shown in Fig. 9 and 10 and confirm the presence of the fracton laws even in the case of combined topological and usual disorder in the magnon equations of motion. It is clear that in this model the states are even more localized, except for the $E \rightarrow 0$ modes.

5. Conclusions

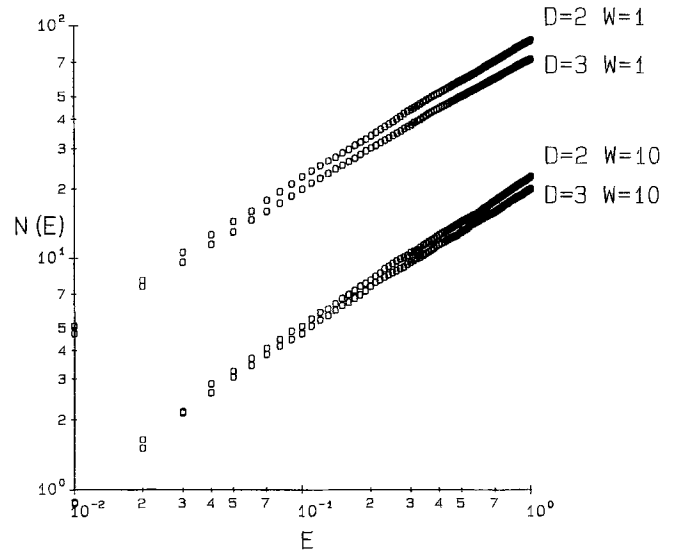We have considered in this paper only spin-wave excitations but our results should also apply unchanged to

phonons $(E = -\omega^2)$ and classical diffusion $(E = i\omega)$. Relevant experimental data for the vibrational problem are summarized in [9–11]. These experimental facts were the main motivation for initiating studies of the dynamics in fractal structures. Our results are in favour of the fracton description in both two and three dimensions. The localization of fractons has been examined also by considering the DOS-fluctuations.

In summary, we have considered the eigensolutions of the infinite percolating cluster of a site-dilute 2- and 3-dimensional Heisenberg ferromagnet for a range of values of the bond concentration p. The method of Lanczos was used to obtain the eigensolutions, being very economical mostly in computer storage requirements. The results obtained are summarized below:

(i) The DOS satisfies closely the Alexander-Orbach scaling, also by including continuous randomness on the bonds of the percolating cluster and the magnon-fracton crossover can also be seen to be smooth, without the presence of a peak.

(ii) The level-statistics of fracton modes reveal a distribution close to exponential (Poisson) which implies strong localization. From the level-statistics in the upper part of the spectrum we find that the fracton modes disappear for concentrations above $p = 0.45$ in $d = 3$, invalidating the scaling picture.

(iii) The fracton amplitudes are seen to have strong decay properties consistent with a scaling description for the averaged values but also accompanied by very large fluctuations. Our results indicate the unusual localization properties of fractons. Future studies will lie on two fronts: First, to distinguish superlocalization from localization and second to determine the crucial mobility edge versus concentration p phase diagram.

References

1. Mandelbrot, B.B.: The fractal geometry of nature. San Francisco: Freeman 1982
2. Stauffer, D.: Introduction to percolation theory. London: Taylor and Francis 1985
3. Havlin, S., ben-Avraham, D.: Adv. Phys. **36**, 695 (1987)
4. Alexander, S., Orbach, R.: J. Phys. (Paris) Lett. **43**, L625 (1982)
5. Stinchcombe, R.B.: In: Scaling phenomena in disordered systems. Pynn, R., Skjeltorp, A. (eds.), p. 13. New York: Plenum Press 1985
6. Evangelou, S.N.: Phys. Rev. **B33**, 3602 (1986)
7. Evangelou, S.N., Papanicolaou, N., Economou, E.N.: Phys. Rev. B **43**, 11171 (1991)
8. Aharony, A., Alexander, S., Entin-Wohlman, O., Orbach, R.: Phys. Rev. **B31**, 2565 (1985)
9. Orbach, R.: Science **231**, 814 (1986)
10. Alexander, S., Laermans, C., Orbach, R., Rosenberg, H.M.: Phys. Rev. **B28**, 4615 (1983)
11. Pfeifer, P., Order, M.: In: The fractal approach to heterogenous chemistry. Avnir, D. (ed.), pp. 11–43). New York: Wiley 1989
12. Rammal, R., Toulouse, G.: J. Phys. (Paris) Lett. **44**, 13 (1983)
13. Kirpatrick, S., Eggarter, T.P.: Phys. Rev. **B6**, 3598 (1972)
14. Levy, Y.E., Souillard, B.: Europhys. Lett. **4**, 233 (1987)
15. Porter, C.E.: Statistical theories of spectra: fluctuations. New York: Academic Press 1965
16. Altshuler, B.L.: Proceedings of the 18th International Conference on Low Temperature Physics. Jpn. J. Appl. Phys. Suppl. **26**, 1938 (1987)
17. Parlett, B.N., Reid, J.K.: AERE Harwell Report No CSS83 (1980); also see Cullum, J.K., Willoughby, R.K.: Lanczos algorithms for large symmetric eigenvalue problems. Boston, Basel, Stuttgart: Birkhauser 1985
18. Hoshen, J., Kopelman, R.: Phys. Rev. **B14**, 3428 (1976)
19. Argyrakis, P.: In: Structure and dynamics of molecular systems. Daudel, R., Korb, J.P., Lemaistre, J.P., Maruani, J. (eds.), pp. 209. Dordrecht: D. Reidel 1986
20. Evangelou, S.N.: Phys. Rev. **B27**, 1397 (1983)
21. Lewis, S.J., O'Brien, M.C.M.: J. Phys. **B18**, 4487 (1985)
22. O'Brien, M.C.M., Evangelou, S.N.: J. Phys. **C6**, 3598 (1980)
23. Altshuler, B.L., Zharekeshev, I.Kh., Kotochigova, S.A., Shklovskii, B.I.: Sov. Phys. JETP **67**, 625 (1988)
24. Bohigas, O., Giannoni, M.J.: Mathematical and computational methods in nuclear physics. Dehesa, J.S., Gomea, J.M., Polls, A. (eds.). In: Lecture Notes in Physics, p. 1. Berlin, Heidelberg, New York: Springer 1984
25. Thouless, D.J.: Phys. Rep. **13**, 93 (1974)
26. Nakayama, T., Yakubo, K., Orbach, R.: J. Phys. Soc. Jpn. **58**, 1891 (1989)